In Situ Electrokinetic Enhancement for Self-Assembled-Monolayer-Based Electrochemical Biosensing

Mandy L. Y. Sin,[†] Tingting Liu,[†] Jeffrey D. Pyne,[†] Vincent Gau,[‡] Joseph C. Liao,[§,∥] and Pak Kin Wong*,[†]

[†]Department of Aerospace and Mechanical Engineering, University of Arizona, Tucson, Arizona 85721, United States
[‡]GeneFluidics Inc, Irwindale, California 91010, United States
[§]Department of Urology, Stanford University, Palo Alto, California 94304, United States
[∥]Veterans Affairs Palo Alto Health Care System, Palo Alto, California 94304, United States

ABSTRACT: This study reports a multifunctional electrode approach which directly implements electrokinetic enhancement on a self-assembled-monolayer-based electro-chemical sensor for point-of-care diagnostics. Using urinary tract infections as a model system, we demonstrate that electrokinetic enhancement, which involves in situ stirring and heating, can enhance the sensitivity of the strain specific 16S rRNA hybridization assay for 1 order of magnitude and accelerate the time-limiting incubation step with a 6-fold reduction in the incubation time. Since the same electrode platform is used for both electrochemical signal enhancement and electrochemical sensing, the multifunctional electrode approach provides a highly effective strategy toward fully integrated lab-on-a-chip systems for various biomedical applications.
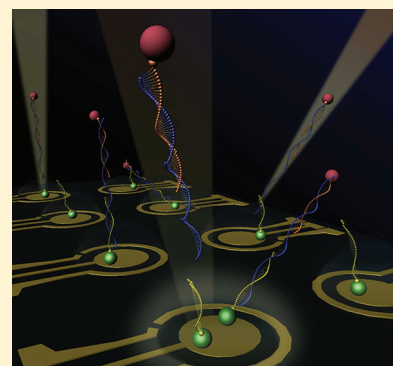
Electrochemical sensing has been one of the most widely adopted detection platforms for biomedical and chemical analyses. Due to its cost-effectiveness, simplicity, and portability, an electrochemical biosensor holds great promise to revolutionize the implementation of point-of-care diagnostics.[1−7] In the past decade, enormous efforts have been devoted to develop electrochemical biosensors for molecular analyses.[8−10] With enzymatic signal amplification, high sensitivity can be achieved by electrochemical sensors without complicated target amplification procedures, such as polymerase chain reaction. This facilitates molecular analyses in decentralized settings with limited supporting equipment and resources. Furthermore, the incorporation of alkanethiol self-assembled monolayer (SAM) including uniform, mixed, and functionalized on the sensor electrodes has been demonstrated to be useful for immobilizing biological components, e.g., nucleic acid sequences, aptamers, and antibodies, as specific molecular recognition elements.[11,12] The SAM also dramatically reduces nonspecific binding on the sensor surface, which in turn improves its specificity and sensitivity.[13] This is critical for eliminating matrix effects and facilitating molecular diagnostics with physiological samples, such as urine and blood.[14,15]

The ultimate performance of electrochemical sensors, however, can often be limited by the diffusion of the target molecule, which is due to the lack of turbulence at small scales,[16−18] and its binding efficiency to the specific recognition element. In fact, the majority of time in most bioanalytical assays is spent on various incubation steps (e.g., probe−target binding and target immobilization on the sensor surface). Without external agitation, long incubation time is required for molecular diffusion and the binding efficiency, i.e., the portion

of the target analyte being captured, is often limited. As a result, most electrochemical biosensors are only effective in applications with high analyte concentration, such as glucose and other blood chemistry.[19,20] For applications with low analyte concentrations, on-chip stirring and heating can potentially improve the performance of the electrochemical sensor and is particularly important for molecular diagnostics at the point of care.

Over the past decade, microscale mixers based on various actuation methods, such as static, centrifugal, ultrasonic, electrokinetic, and magnetic, have been demonstrated.[21−28] However, integrating electrochemical sensors with these mixers, which involve different fabrication procedures, is a challenging task and can significantly increase the complexity and cost of the system. This represents a major hurdle in the realization of the electrochemical sensing on a fully automated lab-on-a-chip system. Among numerous microfluidics sample preparation techniques, electrokinetics is a promising approach for in situ assay enhancement on electrochemical sensors. For example, dc electrokinetics, such as electrophoresis and electro-osmosis, has been demonstrated for various bioanalytical applications.[29,30] However, the requirement of large driving voltage and the formation of bubbles due to electrolysis prevent the implementation of dc electrokinetics for on-chip enhancement. On the other hand, ac electrokinetics requires only a simple electronic interface and low driving voltage, which can avoid bubble formation. For instance, ac electro-osmotic flow has

been applied to generate fluid motion in a microfluidic device.[31] However, ac electro-osmotic flow has a negligible effect at high conductivity (~ 1 S/m) due to the compression of the electrical double layer. This precludes its use in bioanalytical assays that involve high conductivity physiological samples and biological buffers. Alternating current electrothermal flow (ACEF) is another electrohydrodynamic effect, which is highly effective in high conductivity buffers (Figure 1a). In ACEF, when an
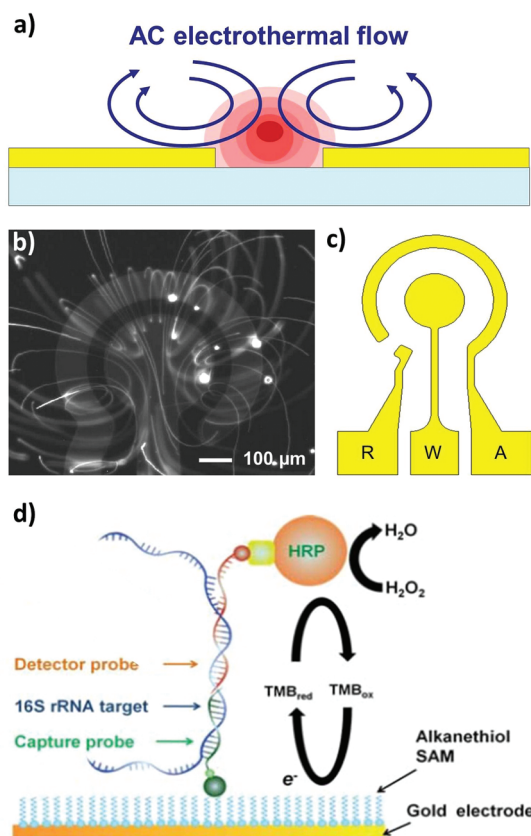

Figure 1. (a) Schematics of ACEF for in situ sensor enhancement. (b) Visualization of the ACEF induced 3D vortices with particle trajectories near the concentric electrode surface in high conductivity buffer ($\sigma = 1$ S/m). (c) The universal electrode design for in situ electrokinetic enhancement and electrochemical pathogen sensing. R, W, and A represent the reference, working, and auxiliary electrodes, respectively. (d) The detection strategy of the electrochemical assay for pathogen detection. The large green circle on top of the alkanethiol SAM represents streptavidin. The small green circle on top of the streptavidin corresponds to the biotin molecule. The small red circle connected to the detector probe corresponds to fluorescein. The yellow square next to the fluorescein corresponds to antifluorescein antibody.

electric field is applied in the fluid, Joule heating can be induced depending on the electrical conductivity of the fluid and the magnitude of the electric field.[32] Nonuniform electric field distribution in the fluid results in temperature gradients near the electrode. The temperature gradient in the medium induces permittivity and conductivity gradients, and the interaction between the electric field and the gradients leads to net electrical force and bulk fluid motion (Figure 1b). ACEF operates at over 100 kHz where electrode polarization and ac electro-osmosis are negligible.[33−35] In a typical microfluidic system, the temperature profile reaches equilibrium on the order of milliseconds, and the effect of ACEF-induced fluid

motion on thermal diffusion is negligible. The energy balance equation can be simplified as[36]

$$k\nabla^2 T + \sigma E^2 = 0 \tag{1}$$

where k, T, and σ are the thermal diffusivity, temperature, and conductivity of the medium, respectively. E is the applied electric field. The temperature rise in the medium due to Joule heating can be estimated by[36]

$$\Delta T = \sigma V_{\mathrm{rms}}^2 / 8k \tag{2}$$

The time-averaged electrothermal force per unit volume has been determined to be[36]

$$\langle f_{\mathrm{E}} \rangle = -\frac{1}{2}\left[\left(\frac{\nabla\sigma}{\sigma} - \frac{\nabla\varepsilon}{\varepsilon}\right)\cdot\vec{E}\frac{\varepsilon\vec{E}}{1 + (\omega\tau)^2} + \frac{1}{2}|\vec{E}|^2\nabla\varepsilon\right] \tag{3}$$

where ω is the angular frequency of the applied electric field, ε is the permittivity of the medium, and $\tau = \varepsilon/\sigma$ is the charge relaxation time of the medium. The first and second terms on the right-hand side of eq 3 represent the Coulomb and the dielectric forces, respectively. In the past, ACEF has been demonstrated to be effective in mixing high conductivity fluids (≥ 1 S/m) and heterogeneous assay enhancement inside microchambers.[33,37,38] Nevertheless, the effects of electro-kinetics on SAM-based electrochemical biosensors has not been investigated systematically, and the applicability of ACEF in manipulating biological and clinical samples has not been demonstrated.

Herein, a multifunctional electrode approach, which implements in situ electrokinetic-induced ACEF stirring and Joule heating directly on a SAM based electrochemical sensor (Figure 1c) for urinary tract infection (UTI) diagnostics, is investigated. The detection strategy of the sandwiched based electrochemical sensors for UTI diagnosis involves the hybridization of the species-specific bacterial 16S rRNA to a biotin-modified capture probe on the sensor surface and a fluorescein-modified detector probe (Figure 1d).[39−43] The enzymatic signal amplification is obtained through the binding of a horseradish peroxidise (POD)-conjugated antifluorescein antibody to the detector probe. The concentration of the target captured on the sensor surface can be quantified by the current obtained through the redox reaction between the tetramethylbenzidine (TMB) and POD. The ability to execute in situ enhancement directly on the sensor surface can maximize the hybridization efficiency of capture probe−target−detector probe complex and allows significant improvement in the sensor performance including an increase in sensor signal, removal of nonspecific binding, reduction in total assay time, and simplification in the sample preparation procedures. Furthermore, the in situ enhancement approach can be applied for manipulating a wide range of samples, including synthetic targets, clinical isolates, and clinical urine samples from patients. Of key importance for the multifunctional approach is that the same electrode platform is used for both on-chip sample preparation and electrochemical sensing without the requirement of complicated system integration procedures.

EXPERIMENTAL SECTION

Bacteria Clinical Isolates and Clinical Urine Specimens. Uropathogenic bacteria clinical isolates including *E. coli*, *S. Saprophyticus*, and *P. aeruginosa* were obtained from Veterans

Affairs Palo Alto Health Care System (VAPAHCS). The clinical urine specimens were collected from patients at Spinal Cord Injury Service at VAPAHCS with approval from the Stanford University institutional review board and informed patient consent. The clinical isolates were received in vials containing Brucella broth with 15% glycerol (BBL, Annapolis, MD) and were stored at −80 °C. The bacteria were grown in Luria broth to logarithmic phase with optical density, OD_{600}, equal to 1 (~1×10^8 cfu/mL). The optical density was measured by a spectrophotometer (Thermo Fisher Scientific, NanoDrop 2000). The samples were frozen in Luria broth with 15% glycerol (BBL, Annapolis, MD) and stored at −80 °C until the time of experimentation.

Oligonucleotide Probe Design. The synthetic target and oligonucleotide probes were synthesized by Integrated DNA Technologies (Coralville, IA). The capture and detector probes were synthesized with 5′ biotin modification and 3′ fluorescein modification, respectively. *E. coli* capture probe (EC471C) and detector probe (EC447D) were designed to hybridize with species-specific regions of the *E. coli* 16S rRNA. The sequence was obtained from the NCBI database (Bethesda, MD), and the hybridization accessibility of the target sequence is evaluated using the Mfold server.[44] In addition to species-specific probe pairs, universal bacterial capture probe (UNI798C) and detector probe (UNI776D) were also designed for Enterobacteriaceae. The universal probe pair was used for detecting *S. Saprophyticus* and *P. aeruginosa*. The sequences of oligonucleotide probes and the synthetic target used are summarized in Table 1.

Table 1. Sequences of Oligonucleotide Used in This Work

oligonucleotide	sequence (5′−3′)
synthetic target	5′-ATGAAGAAGGCCTTCGGGTTGTAAAG TACTTTCAGCGGGGAGGAAGGGAGTAA AGTTAATACCTTTGCTCATTGAC-3′
EC471C	5′-CTGCGGGTAACGTCAATGAGCAAA-3′
EC447D	5′-GGTATTAACTTTACTCCCTTCCTC-3′
UNI798C	5′-TCGTTTACRGCGTGGACTACCA-3′
UNI776D	5′-GGGTATCTAATCCTGTTTGCTC-3′

SAM-Based Electrochemical Sensor. The multifunctional electrodes for both electrokinetic enhancement and electrochemical sensing consist of a reference electrode, a working electrode of 25 mm in diameter, and an auxiliary electrode of 600 μm in width. The gap distance between the working electrode and the auxiliary electrode is 1 mm. The electrodes were deposited by evaporating 120 nm gold on a glass substrate with a 25 nm Ti adhesion layer and were patterned by lift-off. The SAM solution was prepared by mixing 0.218 g of 11-mercaptoundecanoic acid (Sigma-Aldrich, 450561), 682 μL of 6-mercapto-1-hexanol (Sigma-Aldrich, 451088), and 1 L of ethyl alcohol (EMD Chemicals, AX0441-3) on a stirrer (Thermo Scientific, SP195025) at 1000 rpm for 2 h. The layer was self-assembled on the Au electrodes in a mini shaker (VWR, 12620−942) at a speed of 240 rpm for 2 h. The Au electrodes were cleaned with ethyl alcohol (Decon Laboratories, 2701). To activate the carboxyl group of the SAM alkanethiols, the working electrode was incubated in 100 mM of *N*-hydroxysuccinimide (Sigma-Aldrich, 130672) and 400 mM of *N*-3-dimethylaminopropyl-*N*-ethylcarbodiimide (Sigma-Aldrich, E6383) at room temperature for 10 min. The washing steps were performed using deionized water and followed by drying with compressed air. The activated working electrode was incubated in 5 mg/mL biotin (Thermo Scientific, 21346) suspended in 50 mM sodium acetate (Fisher Scientific, BP333) at room temperature for 10 min. The working electrode was then incubated in 4 μL of 1 M ethanolamine (Sigma-Aldrich, 110167) at pH 8.5 at room temperature for 10 min. The pH value was adjusted by addition of hydrochloric acid (Sigma-Aldrich, 320331). The biotinylated working electrode was incubated in 0.5 mg/mL streptavidin (Sigma-Aldrich, S4762) at room temperature for 10 min. The streptavidin-coated working electrode was incubated in 1 μM biotinylated capture probes in 1 M phosphate buffer (Sigma-Aldrich, P3288) at room temperature for 30 min.

Amperometric Detection of Synthetic Target and Bacterial 16S rRNA. For experiments with clinical isolates and clinical urine samples, the 10 μL samples were lysed by 10 μL of lysis buffer consisting of 0.1% Triton X-100 (Sigma-Aldrich, T9 284), 2× Tris-EDTA (Sigma-Aldrich, T9285), and 5 mg/ mL lysozyme (Sigma-Aldrich, L6876) at room temperature for 5 min. Then, 10 μL of 1 M NaOH was added into the solution and incubated at room temperature for 5 min. After lysing the bacteria, 70 μL of the detector probe (0.5 μM) in 1 M phosphate buffer (Sigma-Aldrich, P3288) with 2.5% bovine serum albumin (Sigma-Aldrich, A7906) was added to the bacterial lysate and incubated for 10 min at room temperature. For experiments using synthetic targets, 0.2 nM of the synthetic target was incubated with the detector probe (0.5 μM). The conductivities of the bacterial−lysate−detector probe mixture and the synthetic−target−detector probe mixture were 6 S/m. To detect the target, laser machined plastic wells were bonded to the sensor chip and 50 μL of the mixture was delivered onto the sensor to cover the electrodes. For ACEF, the square wave ac potential was applied across the working and auxiliary electrodes by a function generator (HP, 33210A) once the mixture was delivered on the sensor surface. The signal across the sensor was monitored using a digital oscilloscope (GW Instek, GDS-1102). After washing and drying, 0.5 U/mL antifluorescein horseradish peroxidise (HRP), Fab fragments (Roche, 11426338910) diluted in buffer containing 1:1 volume ratio of stabilZyme HRP conjugate stabilizer (SurModics, SZ02), and 1% (w/v) casein in phosphate-buffered saline (Thermo Scientific, 37528) were deposited on the working electrode and incubated for 15 min. After washing and drying, 50 μL of K-Blue low activity TMB (Neogen, 330176) substrate solution was placed on the sensor to cover the electrodes. Amperometric measurement was taken immediately. The current was measured using a multichannel potentiostat (GeneFluidics Inc.). The voltage was fixed at −200 mV (with respect to the reference electrode), and the electroreduction current was measured at 60 s after the HRP redox reaction reached quasi-steady-state. All data points are reported as mean ± standard deviation for at least three consecutive measurements. Replicates were performed using different sensor electrodes. The limit of detection was estimated by nonlinear curve fitting using SigmaPlot (SigmaPlot Inc.) and was considered to be the blank value (negative control) plus three times the standard deviation of the blank readings (99% confidence).

Microscale Fluorescence Thermometry. For estimating the temperature rise, a two-color fluorescence thermometry technique was used.[45] Two fluorescence dyes, 0.4 mM Rhodamine-B (RhB) (Sigma, 83689) and 26.2 μM Rhodamine-110 (Rh110) (Sigma, 83695), were mixed in the

hybridization buffer with a conductivity of 6 S/m. RhB, which is a temperature sensitive dye, has absorption and emission peaks at 554 and 575 nm, respectively. The temperature sensitivity of RhB is ~1.05% intensity change per K. Rh110 has an absorption peak at 496 nm and an emission peak at 520 nm, and its temperature sensitivity is ~0.08% intensity change per K. Since Rh110 is relatively temperature insensitive, it can normalize for variations in light intensity and fluid concentration. Both dyes are excited by a mercury arc lamp (X-Cite 120Q, EXF0). A dual band excitation filter set (Nikon, FITC-TRITC) is applied for simultaneous detection of emission from both dyes. Band pass excitation and emission filters allow two signal channels, one corresponding to specific narrow regions of blue excitation and green emission (Rh110), and the other to green excitation and orange-red emission (RhB). A three CCD (Toshiba, IK-TF7) color camera is used to separate the emission wavelengths between the dyes, which exports a RGB image file where the red channel represents RhB emission and the green channel represents Rh110 emission. The red and green channel of the color image were extracted and analyzed with ImageJ.

RESULTS AND DISCUSSION

The in situ electrokinetic enhancement approach was first characterized using synthetic targets suspended in hybridization buffer with a conductivity of 6 S/m. The voltage dependence of the hybridization efficiency of the target−detector probe hybrid to the capture probe on the sensor surface was studied with an incubation time of 5 min. The amperometric signal generally increases with the applied voltage while the background level was observed to decrease in a voltage-dependent manner (Figure 2a). While a higher voltage can create stronger electrokinetic effects for facilitating target hybridization, the excessive heat generation and electrochemical reaction may result in sensor damage. In fact, significant fluid evaporation and sensor damage are observed at high voltage (e.g., 6 V_{pp}) with a long incubation time. Furthermore, a high temperature approaching the melting temperature could induce thermal denaturation. Therefore, the applied voltage is chosen to be 5 V_{pp}. Examining the voltage dependence of the electrochemical signal by subtracting the diffusion component reveals that ACEF enhancement displays a power exponent of 2.8 ± 0.5 (i.e., $\sim V^{2.8\pm0.5}$). This is moderately lower than the fourth power dependence expected for ACEF. Nevertheless, this is in agreement with the dependence of ACEF fluid velocity measured at a similar conductivity and can be understood by the nonlinear nature of the electrochemical sensor signal.[37] This supports the hypothesis that ACEF can enhance the capture efficiency by transporting the targeting molecules to the sensor surface. In addition, we have also examined the frequency dependency on the ACEF enhancement approach. The amperometric signal levels remain constant in the frequency range from 200 kHz to 15 MHz (data not shown). Since ACEF is independent of the applied frequency in this range (the crossover frequency is ~8 GHz at 6 S/m), the observation further supports that the enhancement is a result of ACEF in contrast to other electrokinetic phenomena such as dielectrophoresis or ac electro-osmosis, which have strong frequency dependencies in this range.

In order to study the effect of in situ enhancement on the hybridization kinetics, the sensor performance with diffusion was compared to the result with ACEF at different times. The incubation time by diffusion was examined from 2 to 35 min. A
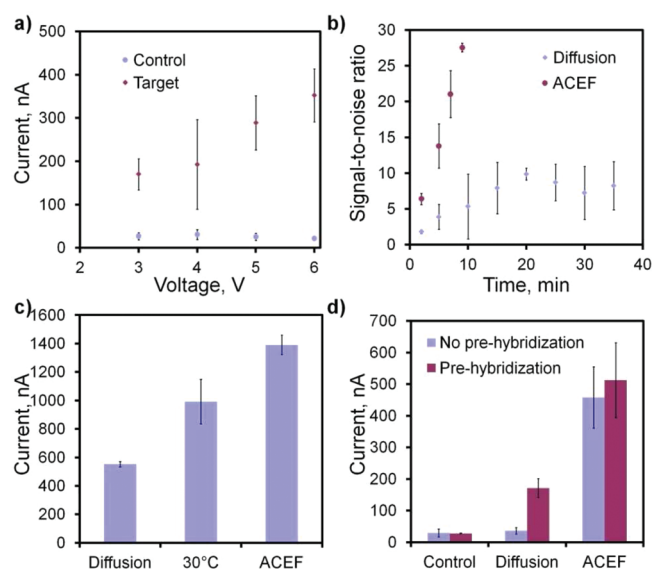

Figure 2. (a) Voltage dependence of the electrochemical sensor signal with in situ ACEF enhancement. A square wave ac signal at 200 kHz was applied across the working and auxiliary electrodes for 5 min. (b) Comparison of the sensor performances using 0.2 nM of synthetic target with and without ACEF enhancement at different times. The applied ac potential was 5 V_{pp} at 200 kHz. (c) Investigation of the relative importance of ACEF-induced heating with ACEF-induced advection using E. coli clinical isolates at a concentration of 1×10^6 cfu/mL. Three conditions were tested including incubation at room temperature (20 °C), incubation on a hot plate at 30 °C, and ACEF enhancement (square wave at 5 V_{pp} and 200 kHz) with an incubation time of 8 min. (d) Comparison of the amperometric sensor signal with and without the prehybridization step of the bacterial lysates and detector probes. The incubation time is 8 min.

shorter range of incubation time, 2−10 min, was studied with ACEF as a long incubation time with electrokinetic enhancement could cause significant fluid evaporation and lower the signal ultimately. With diffusion, the signal-to-noise level reaches equilibrium in approximately 20 min. With ACEF, the time required to reach a similar signal-to-noise level is 3 min, which is over 6-fold reduction in the incubation time. As also shown in Figure 2a, we observed both signal enhancement and background reduction with ACEF, which results in a significant improvement in the signal-to-noise ratio compared to diffusion (Figure 2b). The background reduction can be understood by the fluid motion and the Joule heating-induced temperature rise that remove the nonspecific molecular binding and lower the background noise. The increase in sensor signal is contributed by the molecular advection induced by ACEF, which improves the efficiency for capturing the target on the sensor surface. To further illustrate this point, we estimate the relative importance between ACEF-induced advection and diffusive transportation in the electrochemical sensor by considering the Péclet number ($Pe = uL/D$), where u is the ACEF velocity (100 μm/s), L is the length scale of the system (1 mm), and D is the diffusion coefficient of the synthetic target (4×10^{-7} cm²/s). The Péclet number is on the order of 1000, which supports the importance of ACEF-induced advection for assay enhancement. It should also be noted that the synthetic target has a higher diffusivity compared to the bacterial 16S rRNA, and therefore, the reduction in incubation time could be even higher for pathogen detection.

The temperature rise due to Joule heating can also contribute to the enhanced signal of the sensor signal by facilitating the hybridization reaction. Therefore, the relative significance of ACEF induced advection to Joule heating on the assay enhancement is investigated. The temperature of the hybridization buffer can reach 30 °C at 5 V_{PP} with a buffer conductivity of 6 S/m. As the melting temperature of the capture and detector probes studied ranges from 52.5 to 59.9 °C, which is at least 20 °C larger than ACEF induced temperature rise, it is anticapted that Joule heating effect will not promote the denaturation between targets and probes. To study the relative contribution of the Joule heating effect, the hybridization steps were performed on a hot plate set at 30 °C and at room temperature (Figure 2c). Uropathogenic E. coli clinical isolates at 1×10^6 cfu/mL were used in the experiment as the model pathogens. Increasing the temperature from 20 to 30 °C significantly increases the sensor signal. Remarkably, the sensor signal with electrokinetic enhancement is ~30% higher than the one based on diffusion at 30 °C. These data suggest that the enhancement cannot be fully explained by the temperature effect and both fluid advection and Joule heating contribute to the electrokinetic enhancement. With ACEF-induced advection, the molecules far away from the electrode can be effectively transported to the senor surface for increasing the target capture efficiency. At the same time, the Joule heating-induced temperature rise near the sensor surface enhances molecular diffusion and facilitates the target hybridization reaction by providing thermal energy to overcome the reaction energy barrier.

In addition to the target−capture probe hybridization step, the applicability of electrokinetic enhancement for the target-detector probe hybridization step is also tested as hybridization is the most time-consuming step in the electrochemical assay (Figure 2d). In this experiment, the signals based on diffusion at room temperature and ACEF with and without a 10 min target−detector probe prehybridization step at room temperature are compared. Without prehybridization, the sensor signal is low and comparable to the background level. The signal with electrokinetic enhancement is significantly higher than the signals based on diffusion with and without prehybridization. With ACEF enhancement, the experiments with and without prehybridization have resulted in similar signal levels that cannot be distinguished statistically. The signal is 14-fold higher than the signal by diffusion without prehybridization. This result suggests that ACEF can significantly enhance the hybridization of the capture probe−target−detector probe complex in a single step effectively without prehybridization. The electrokinetic enhancement approach allows the sample preparation procedures to be simplified and presents a pathway to automate the electrochemical assay.

We further characterized the sensor performance by studying the limit of detection (LOD) of the assay based on diffusion at room temperature and electrokinetic enhancement using uropathogenic E. coli clinical isolates with concentrations ranged from 1×10^4 cfu/mL to 1×10^6 cfu/mL, which is the clinically relevant range for UTI detection. As illustrated in Figure 3a, the signal with electrokinetic enhancement is higher than the signal based on diffusion. We also consistently observe a lower background signal with electrokinetic enhancement. The background reduction can be understood by the combination of temperature rise and fluid motion, which removes the nonspecifically bound molecules. Both increase in signal and reduction in background levels contribute to the
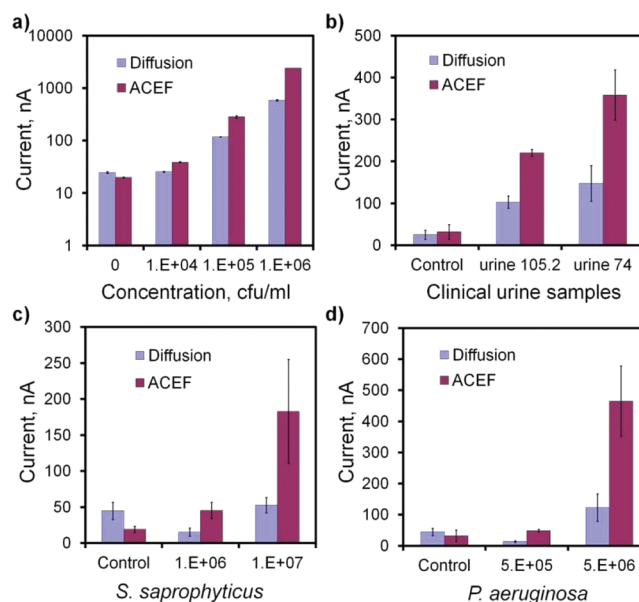

Figure 3. Comparison of the sensor performance based on diffusion and ACEF enhancement (square wave potential of 5 V_{PP} and 200 kHz) with an incubation time of 8 min for detecting (a) different concentrations of E. coli clinical isolates in culture media, (b) E. coli in clinical samples urine 105.2 and urine 74 with 4×10^4 cfu/mL and 4×10^6 cfu/mL E. coli, respectively, (c) S. saprophyticus clinical isolates, and (d) P. aeruginosa clinical isolates.

overall electrokinetic enhancement and improve the overall LOD of the electrochemical sensor. The LOD with electrokinetic enhancement is estimated to be 6.11×10^3 cfu/mL, which is a 1 order of magnitude improvement compared to diffusion.

A major challenge in clinical diagnostics is the matrix effect in physiological samples. To be applicable in UTI diagnostics, electrokinetic enhancement should be compatible with urine samples from patients. To evaluate the applicability of electrokinetic enhancement in urine, we performed the experiment with two clinical urine samples from patients with UTI and compared the signals with and without electrokinetic enhancement. The urine samples have been determined to have 4×10^4 cfu/mL and 4×10^6 cfu/mL E. coli, respectively. As shown in Figure 3b, electrokinetic enhancement increases the signal levels for both samples without significantly affecting the background from the urine without bacteria (control). This demonstrates the applicability of in situ electrokinetic enhancement in UTI diagnostics. In addition to E. coli, other common uropathogens including Pseudomonas aeruginosa (P. aeruginosa) and Staphylococcus saprophyticus (S. saprophyticus) were also tested. As shown in Figure 3c,d, electrokinetic enhancement is able to enhance the signal level for the clinical isolates of both uropathogens. These results support the general applicability of electrokinetic enhancement in pathogen detection and potentially other electrochemical sensing applications.

■ CONCLUSIONS

SAM-based electrochemical sensing has been proven to be an attractive platform for point-of-care diagnostics due to its simplicity and portability. Our work presents a novel approach, which implements electrokinetic enhancement directly on SAM-based electrochemical sensors. The advantage of this multifunctional electrode strategy over other existing mixing

and on-chip heating schemes is the simplicity in system integration, in which the same electrode platform is used for both on-chip enhancement and sensing. This efficient approach enhances the hybridization efficiency of capture probe−target−detector probe complex and allows significant improvement on the sensor performance including 1 order of magnitude decrease in the limit of detection, reduction in the total assay time on the universal electrode platform, and the simplification of sample preparation procedures. Also, the technique is applicable to various types of samples, including synthetic targets, clinical isolates, and clinical urine samples with the concentration range that is clinically relevant to UTI diagnostics. Since molecular advection and molecular binding efficiency are the fundamental limiting factors that are commonly observed in various biomedical assays, electrokinetic enhancement is anticipated to benefit other sensing platforms toward a wide spectrum of clinical and biochemical applications.

■ AUTHOR INFORMATION

Corresponding Author

*Phone: +1-520-626-2215. Fax: +1-520-621-8191. E-mail: pak@email.arizona.edu.

Notes

The authors declare no competing financial interest.

■ ACKNOWLEDGMENTS

■ REFERENCES

(1) Gabig-Ciminska, M. *Microb. Cell Fact.* **2006**, 5.

(2) Liu, R. H.; Yang, J. N.; Lenigk, R.; Bonanno, J.; Grodzinski, P. *Anal. Chem.* **2004**, 76, 1824−1831.

(3) Wang, J. *Nucleic Acids Res.* **2000**, 28, 3011−3016.

(4) Wang, J. *TrAC,-Trends Anal. Chem.* **2002**, 21, 226−232.

(5) Wang, J. *Biosens. Bioelectron.* **2006**, 21, 1887−1892.

(6) Wang, J.; Kawde, A. B. *Analyst* **2002**, 127, 383−386.

(7) Drummond, T. G.; Hill, M. G.; Barton, J. K. *Nat. Biotechnol.* **2003**, 21, 1192−1199.

(8) Mach, K. E.; Mohan, R.; Baron, E. J.; Shih, M. C.; Gau, V.; Wong, P. K.; Liao, J. C. *J. Urol.* **2011**, 185, 148−53.

(9) Pan, Y.; Sonn, G. A.; Sin, M. L.; Mach, K. E.; Shih, M. C.; Gau, V.; Wong, P. K.; Liao, J. C. *Biosens. Bioelectron.* **2010**, 26, 649−54.

(10) Mach, K. E.; Du, C. B.; Phull, H.; Haake, D. A.; Shih, M. C.; Baron, E. J.; Liao, J. C. *J. Urol.* **2009**, 182, 2735−2741.

(11) Wink, T.; van Zuilen, S. J.; Bult, A.; van Bennkom, W. P. *Analyst* **1997**, 122, 43R−50R.

(12) Husemann, M.; Mecerreyes, D.; Hawker, C. J.; Hedrick, J. L.; Shah, R.; Abbott, N. L. *Angew. Chem., Int. Ed.* **1999**, 38, 647−649.

(13) Nath, N.; Hyun, J.; Ma, H.; Chilkoti, A. *Surf. Sci.* **2004**, 570, 98−110.

(14) Chiu, M. L.; Lawi, W.; Snyder, S. T.; Wong, P. K.; Liao, J. C.; Gau, V. *JALA* **2010**, 15, 233−242.

(15) Sviridov, D.; Hortin, G. L. *Clin. Chim. Acta* **2009**, 404, 140−3.

(16) Meldrum, D. R.; Holl, M. R. *Science* **2002**, 297, 1197−1198.

(17) Stone, H. A.; Stroock, A. D.; Ajdari, A. *Annu. Rev. Fluid Mech.* **2004**, 36, 381−411.

(18) Ho, C. M.; Tai, Y. C. *Annu. Rev. Fluid Mech.* **1998**, 30, 579−612.

(19) Newman, J. D.; Turner, A. P. F *Biosens. Bioelectron.* **2005**, 20, 2435−2453.

(20) Tsai, M. Y.; Schwichtenberg, K.; Tuchman, M. *Clin. Chem.* **1993**, 39, 280−283.

(21) Kamio, E.; Ono, T.; Yoshizawa, H. *Lab Chip* **2009**, 9, 1809−1812.

(22) Yan, D. G.; Yang, C.; Miao, J. M.; Lam, Y. C.; Huang, X. Y. *Electrophoresis* **2009**, 30, 3144−3152.

(23) Biddiss, E.; Erickson, D.; Li, D. Q. *Anal. Chem.* **2004**, 76, 3208−3213.

(24) Huang, M. Z.; Yang, R. J.; Tai, C. H.; Tsai, C. H.; Fu, L. M. *Biomed. Microdevices* **2006**, 8, 309−315.

(25) Noroozi, Z.; Kido, H.; Micic, M.; Pan, H. S.; Bartolome, C.; Princevac, M.; Zoval, J.; Madou, M. *Rev. Sci. Instrum.* **2009**, 80.

(26) Rife, J. C.; Bell, M. I.; Horwitz, J. S.; Kabler, M. N.; Auyeung, R. C. Y.; Kim, W. J. *Sens. Actuators, A* **2000**, 86, 135−140.

(27) Lee, S. H.; van Noort, D.; Lee, J. Y.; Zhang, B. T.; Park, T. H. *Lab Chip* **2009**, 9, 479−482.

(28) Wang, Y.; Zhe, J.; Chung, B. T. F.; Dutta, P. *Microfluid. Nanofluid.* **2008**, 4, 375−389.

(29) Sosnowski, R. G.; Tu, E.; Butler, W. F.; O'Connell, J. P.; Heller, M. J. *Proc. Natl. Acad. Sci. U.S.A.* **1997**, 94, 1119−1123.

(30) Heller, M. J. *Annu. Rev. Biomed. Eng.* **2002**, 4, 129−153.

(31) Wong, P. K.; Chen, C. Y.; Wang, T. H.; Ho, C. M. *Anal. Chem.* **2004**, 76, 6908−6914.

(32) Gonzalez, A.; Ramos, A.; Morgan, H.; Green, N. G.; Castellanos, A. *J. Fluid Mech.* **2006**, 564, 415−433.

(33) Feldman, H. C.; Sigurdson, M.; Meinhart, C. D. *Lab Chip* **2007**, 7, 1553−1559.

(34) Gao, J.; Sin, M. L. Y.; Liu, T.; Gau, V.; Liao, J. C.; Wong, P. K. *Lab Chip* **2011**, 11, 1770−1775.

(35) Park, S.; Koklu, M.; Beskok, A. *Anal. Chem.* **2009**, 81, 2303−2310.

(36) Ramos, A.; Morgan, H.; Green, N. G.; Castellanos, A. *J. Phys. D: Appl. Phys.* **1998**, 31, 2338−2353.

(37) Sin, M. L. Y.; Gau, V.; Liao, J. C.; Wong, P. K. *JALA* **2010**, 15, 426−432.

(38) Ng, W. Y.; Goh, S.; Lam, Y. C.; Yang, C.; Rodriguez, I. *Lab Chip* **2009**, 9, 802−809.

(39) Gau, J. J.; Lan, E. H.; Dunn, B.; Ho, C. M.; Woo, J. C. S. *Biosens. Bioelectron.* **2001**, 16, 745−755.

(40) Gau, V.; Ma, S. C.; Wang, H.; Tsukuda, J.; Kibler, J.; Haake, D. A. *Methods* **2005**, 37, 73−83.

(41) Liao, J. C.; Mastali, M.; Gau, V.; Suchard, M. A.; Moller, A. K.; Bruckner, D. A.; Babbitt, J. T.; Li, Y.; Gornbein, J.; Landaw, E. M.; McCabe, E. R. B.; Churchill, B. M.; Haake, D. A. *J. Clin. Microbiol.* **2006**, 44, 561−570.

(42) Liao, J. C.; Mastali, M.; Li, Y.; Gau, V.; Suchard, M. A.; Babbitt, J.; Gornbein, J.; Landaw, E. M.; McCabe, E. R. B.; Churchill, B. M.; Haake, D. A. *J. Mol. Diagn.* **2007**, 9, 158−168.

(43) Lawi, W.; Wiita, C.; Snyder, S. T.; Wei, F.; Wong, D.; Wong, P. K.; Liao, J. C.; Haake, D. A.; Gau, V. *JALA* **2009**, 14, 407−412.

(44) Zuker, M. *Nucleic Acids Res.* **2003**, 31, 3406−3415.

(45) Funatani, S.; Fujisawa, N.; Ikeda, H. *Meas. Sci. Technol.* **2004**, 15, 983−990.